

Bacterial biomass production and ammonium regeneration in Mediterranean sea water supplemented with amino acids. 2. Nitrogen flux through heterotrophic microplankton food chain

F. Van Wambeke & M. A. Bianchi

Laboratoire de Microbiologie du Milieu Marin, C.N.R.S., ER 223, Université de Provence, F-13 331 Marseille Cedex 3, France

ABSTRACT: Nitrogen dynamics effected by bacteria and bacterivorous microflagellates were investigated in a 350 l batch experiment. In conditions favouring heterotroph activity (initial amino-acid enrichment $100 \mu\text{g-at N l}^{-1}$) mineralization rates were respectively 2.7 and $10 \mu\text{g-at N-NH}_4^+ \text{ l}^{-1}$ ($\text{mg dry weight}^{-1} \text{ h}^{-1}$) for bacteria and heterotrophic microflagellates. Heterotrophic bacterial community dynamics were investigated by hierarchical classifications, catabolic potentialities and Shannon diversity indexes. Amino-acid enrichments favoured the development of 2 heterotrophic bacterial communities with complementary physiological roles. One, with growth factor requirements, was able to degrade macromolecules; the other possessed high abilities to use small organic compounds as amino acids. Qualitative composition evolution was correlated to changes in biotic and abiotic parameters.

INTRODUCTION

Aerobic mineralization of amino acids in natural aquatic environments is an example of a process involving structural as well as functional evolutions of communities (Hollibaugh et al. 1980, Iturriaga & Zsolnay 1981, Sepers 1981, Bright & Fletcher 1983, Van Wambeke et al. 1983). In such nitrogen flux, positive and negative interactions (e.g. mutualism, predation, inhibitors) have to be considered through the different components of the system.

While numerous papers deal with nitrogen behaviour through bacterial communities by considering C/N ratios and NH_4^+ fluxes (Amano et al. 1982, Graham & Canale 1982, Laake et al. 1983), others deal more precisely with interactions between bacteria and microflagellates with classical predator-prey considerations (Fenchel 1982, Graham & Canale 1982, Laake et al. 1983); only a few studies deal with the influence of Protozoa on microbial activity or the qualitative composition on bacteria or *vice versa* (Gude 1979, Sherr et al. 1982, Sherr et al. 1983).

Quantitative evolutions of biotic and abiotic parameters were previously considered during bacterial

growth resulting from amino-acid enrichment of natural waters (Van Wambeke & Bianchi 1985). In considering the first 2 communities involved in nitrogen transport from the initial source of dissolved organic matter, i.e. heterotroph bacteria and flagellates, we examined the influence of the qualitative composition of heterotrophic bacterial communities on nitrogen evolution. In the case of a heterotroph-favouring system, values of clearance, biomass yield and ammonium regeneration were produced.

Taxonomic diversity, physiological capacities and nutrient utilization capacities of heterotroph bacterial communities were examined in a 10 d batch-system study of natural sea water enriched with amino acids.

METHODS

A sea-water sample from an oligotrophic area of the Gulf of Marseille (France) was divided into 350 l batches, in open air, as previously described (Van Wambeke & Bianchi 1985). The 'enriched batch' was initially enriched with $30 \mu\text{g-at N-amino acids l}^{-1}$. The 'control batch' was initially enriched with $30 \mu\text{g-at N-}$

NH_4^+ 1^{-1} . The blank was not enriched. The experiment started at 10 a.m. on January 20.

Sampling times differed according to the water volume required for parameter measurements, varying from 0.5 h to 1d.

Quantitative studies. Bacteria and flagellates were enumerated by acridine orange direct counts (AODC; method of Hobbie et al. 1977). For bacteria and flagellates, 0.1 to 0.5 ml and 3 to 4 ml of the sample were stained, respectively. For bacteria, the volume was calculated according to the formula of Krambeck et al. (1981); bacterial carbon content was calculated from direct counts and average cell volume (VOL): bacterial carbon = AODC \times VOL \times density \times carbon/wet weight ratio. The density value is 1×10^{-9} mg μm^{-3} and the carbon/ww ratio is 0.1. Volumes of flagellates were calculated, assuming these represented spheres.

1 to 5 l of the sample were filtered through a 25 mm Whatman GF/C glass-fibre filter which had been preashed for one night at 400 °C. The filters were stored at -20 °C and then oven-dried at 60 °C prior to analysis for particulate carbon and nitrogen in a Perkin Elmer analyser calibrated with acetanilide.

For pigments, 250 ml sample were filtered through 47 mm Whatman GF/C filters with magnesium carbonate 1 % w/v and stored at -20 °C in the dark. After acetone extraction, chlorophyll *a* and phaeopigments were measured before and after acidification on the fluorimeter (Yentch & Menzel, 1963). NH_4^+ and PO_4^{--} were measured according Strickland & Parsons (1968).

Qualitative studies of heterotroph bacterial com-

Table 1. Sampling times of qualitative study

T0	0d 0h	T3	2d 18h	T6	4d 3h	T9	10d
T1	1d 12h	T4	3d 9h	T7	5d 18h		
T2	2d 6h	T5	3d 21h	T8	8d		

munities. In order to describe the qualitative evolution of heterotroph bacteria during the experiment we decided to: (1) compare bacterial evolution among all batches at different sampling times, using synthetical indices as diversity index and physiological indexes; (2) show how the qualitative evolution was performed in each batch comparing all strains isolated from 1 batch at all sampling times.

Strain collection: the samples chosen for these studies were those exhibiting great changes in bacterial numbers. For this reason the period between 2 successive samples was not always the same (Table 1). In each sample, 20 colonies were picked at random from Oppenheimer & ZoBell (1952) plate counts, incubated at 20 °C. Pure strains were described by 100 morphological, biochemical, physiological and nutritional features (Van Wambeke et al. 1985). Results are coded in binary form (1 or 0). A total of 200 strains per batch were isolated and compared in 2 ways: sample by sample or all together.

Diversity indexes. The 20 isolated strains per sample were submitted to hierarchical classification: Jaccard's coefficient for similarity and average distance for linkage. Ecological profiles were determined from clusters at 70 % similarity (Mills & Wassel 1980, Bianchi & Bianchi 1982). The Shannon diversity index ($H = -\sum \text{pi} \log_2 \text{pi}$ (here pi = percentage of the total number of strains in the *i*th profile) was estimated for each sample. Maximal theoretical diversity for the 20 strains studied is $H_{\text{max}} = \log_2 (20) = 4.32$; minimum theoretical value is zero.

Physiological indexes. We established the exoenzyme average index possession (EAI) and the average index of carbonaceous compounds utilisation (UAI) corresponding to the 38 substrates tested as being the sole source of carbon and energy. Average indexes of amino acids (AAI), carbohydrates (CAI), alcohols (OAI), fatty acids (FAI), organic acids of intermediary

Table 2. List of compounds in each chemical group studied and corresponding average index utilization code

Carbohydrates (CAI)	Amino acids (AAI)	Fatty acids (FAI)	Alcohols (OAI)	Organic acids (KAI)	Exoenzymes (EAI)
Arabinose	Proline	Acetate	Mannitol	Malonate	Urease
Ribose	Tryptophan	Propionate	Sorbitol	Succinate	Phosphatase
Glucose	Glycine	Butyrate	Glycerol	Fumarate	Esculinase
Lactose	Alanine	Caproate		Citrate	Tweenase
Sucrose	Serine			α ketoglutarate	Lecithinase
Starch	Aspartate			Glycolate	Amylase
Gluconate	Glutamate			Lactate	DNase
N-acetylglucosamine	Lysine				
	Arginine				
	Ornithine				
	Asparagine				
	Methionine				

metabolism (KAI) were also set (Table 2). They were calculated as follows: $ZAI = (\Sigma+ \times 100)/(n \times \Sigma Z)$, where $\Sigma+$ = positive responses in the Z family for all strains of the sample; n = number of strains of the sample; ΣZ = number of compounds tested in the Z family.

Batch evolution. The 200 strains of each batch were submitted to another hierarchical classification. Similarity (CHI square distance) and clustering (variance algorithm) were calculated according to Delabre et al. (1973).

Grazing and growth. Bacterial growth rates were calculated from the exponential part of the growth curves, and extrapolated from regression analysis on the curves $\ln(\text{direct counts}) = f(\text{time})$. Gross growth efficiency, E , was also determined by calculating the amount of protozoan biovolume produced from the bacterial biomass, $E = Pf (Bi - Bf) \times 100$, where Pf and Bi = respectively maximum flagellate and bacterial biomasses in $\mu\text{m ml}^{-1}$; Bf = final bacterial biomass per ml in the batch.

Clearance, F , was calculated from the equation of Frost (1972): $F = gV/N$, where g = grazing rate; V = volume of the batch; N = average number of flagellates during exponential growth. To account for the grazer's 50% growth during the sample time interval, N was calculated by the equation $N = (Nt - N_0)/(\ln Nt - \ln N_0)$ (Heinbokel 1978). Ingestion rates varied according to bacterial concentrations and were calculated at different time intervals.

RESULTS

Quantitative results

Although the average temperature was 10°C during the experiment, 10 d were sufficient to observe a complete heterotrophic succession in our system. Bacterial numbers increased from 0.3 to 30×10^6 bacteria ml^{-1} in the enriched batch, and to 5 and 7×10^6 bacteria ml^{-1} in the blank and in the control batch, respectively, until 2 d 8 h. Microflagellates grew from Days 5 to 6 or 7, depending on the batches, and then decreased (Fig. 1).

The decrease of pheopigments from 47% to 10–30% (Fig. 2) during the first 2 d documented the stressed state of the phytoplankton at the beginning of the experiment, and its progressive return to a better physiological state. In the amino-acid enriched batch (highest bacterial number) the chlorophyll value was more important and the pheopigment percentage was lower than in other batches. Furthermore, phytoplankton developed less well in the NH_4^+ batch than in the blank batch suggesting a negative initial effect of the

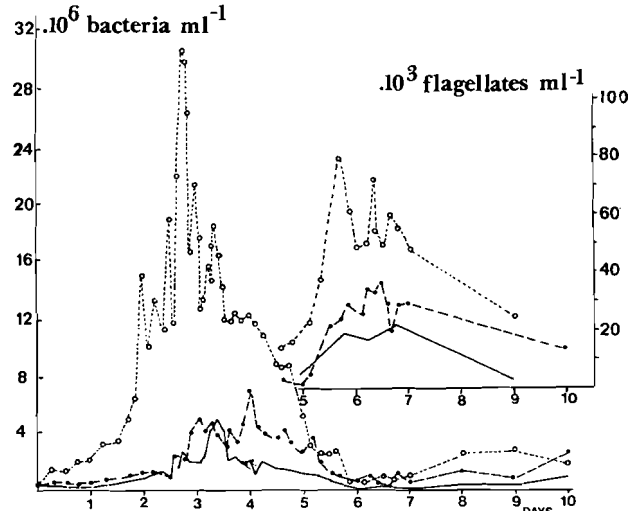


Fig. 1. Direct counts of bacteria and flagellates in amino-acid (o) and NH_4^+ (•) enriched batches, and in the blank batch (solid lines)

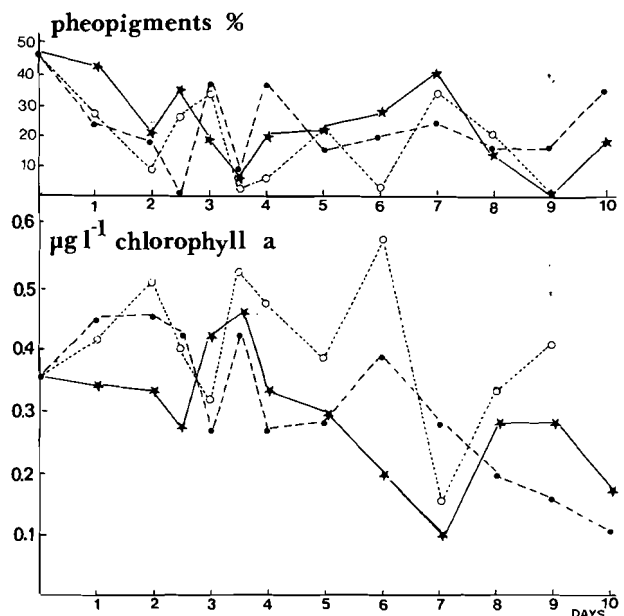


Fig. 2. Chlorophyll a contents on $0.45 \mu\text{m}$ filters and phaeopigment percentages in amino acids (o) and NH_4^+ (•) batches, and in the blank batch (solid lines)

high N/P ratio ($30/0.6 = 50$) on the phytoplankton community.

N-ammonia salt was not assumed to limit growth, except in the blank batch, unlike the dissolved phosphates (Fig. 3) which were all in an organic form at Day 5. NH_4^+ accumulation in the enriched batch revealed mineralization activities (Fig. 4), and high NH_4^+ assimilation was observed over a 10 d period in the control batch, even without phytoplankton.

Particulate carbon and nitrogen (Fig. 5) increased simultaneously during the experiment. The particulate

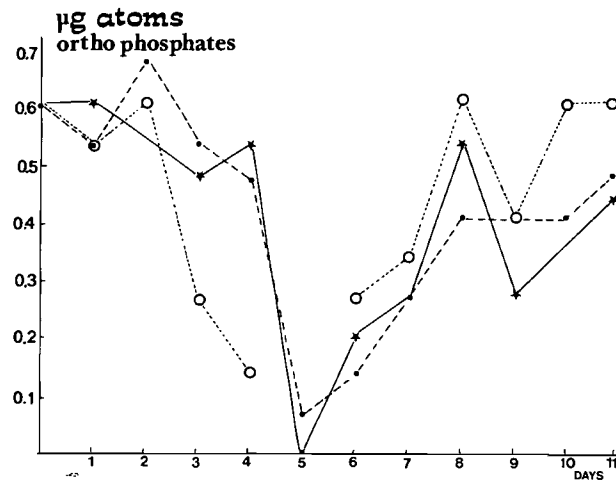


Fig. 3. Total (dissolved and particulate) orthophosphates in amino-acid (○) and NH₄⁺ (●) enriched batches, and in the blank batch (★)

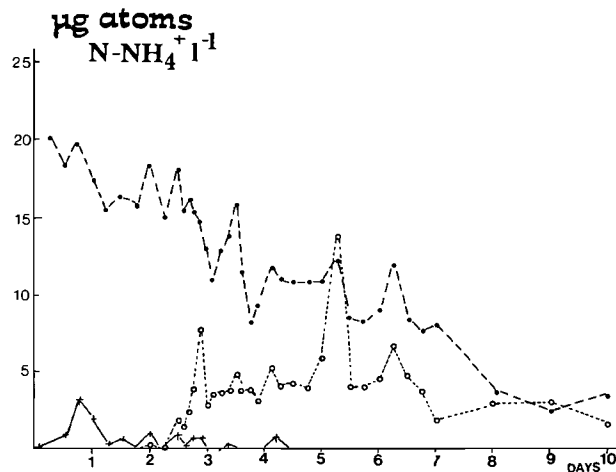


Fig. 4. NH₄⁺ measured in amino-acid (○) and NH₄⁺ (●) enriched batches, and in the blank batch (+)

C/N results revealed a different contribution of bacterial number and average bacterial cell volume, to the carbon measurements in the enriched batch. Estimated bacterial carbon calculated from direct count measurements and average cell volume are plotted Fig. 6. The first great increase in particulate carbon between Day 1 and Day 2 can be explained by the average cell volume increase from 0.1 to 0.2 µm³, while bacterial numbers did not vary very much during this phase. But, when direct counts reached maxima values, particulate carbon did not show a peak because average bacteria cell volume was decreasing. The particulate carbon maximum was noticed on Day 4, when the average cell volume increased again (0.25 µm³), while bacterial numbers were still 12.6 × 10⁶ bacteria ml⁻¹.

Diversity indexes

The Shannon diversity index was 4.22 (Fig. 7b) at T0, characterizing a very diversified initial community. During the bacterial exponential growth phase, there was a decrease of the Shannon index from T0 to T3 in

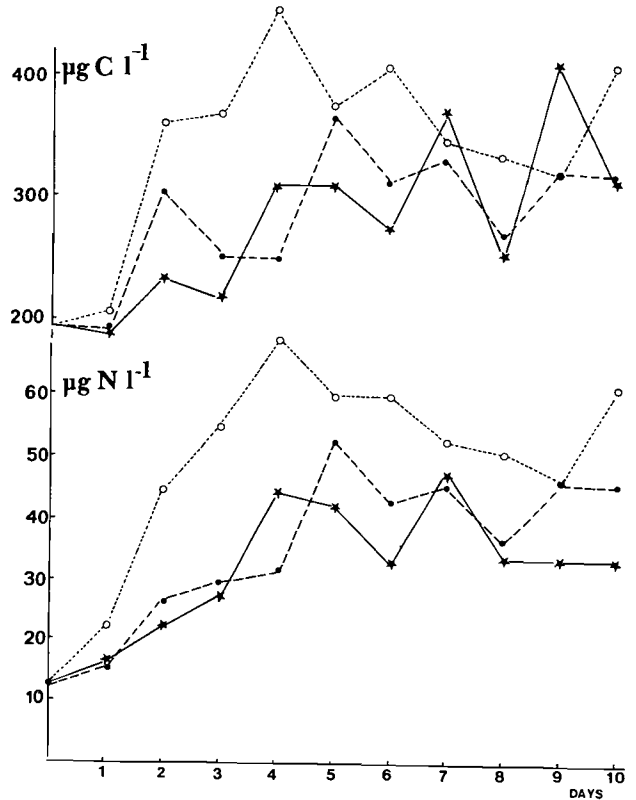


Fig. 5. Particulate nitrogen and carbon in amino-acid (○) and NH₄⁺ (●) enriched batches, and in the blank batch (★)

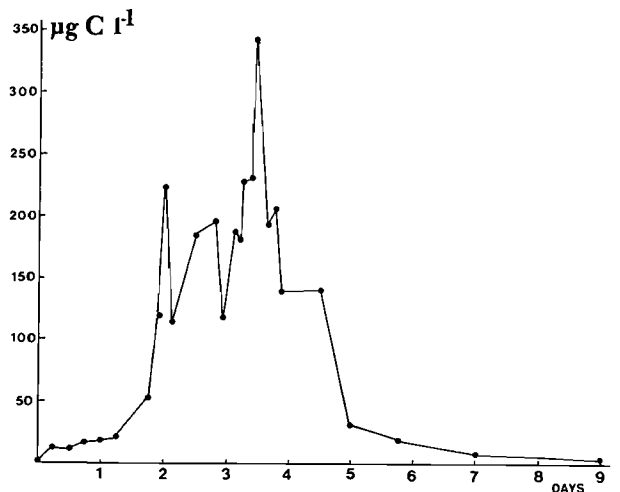


Fig. 6. Carbon contents estimated from acridine orange direct counts, biovolume measurements on photographs, density 1 × 10⁻⁹ mg µm⁻³, and carbon/wet weight ratio 0.1 in the amino-acid enriched batch

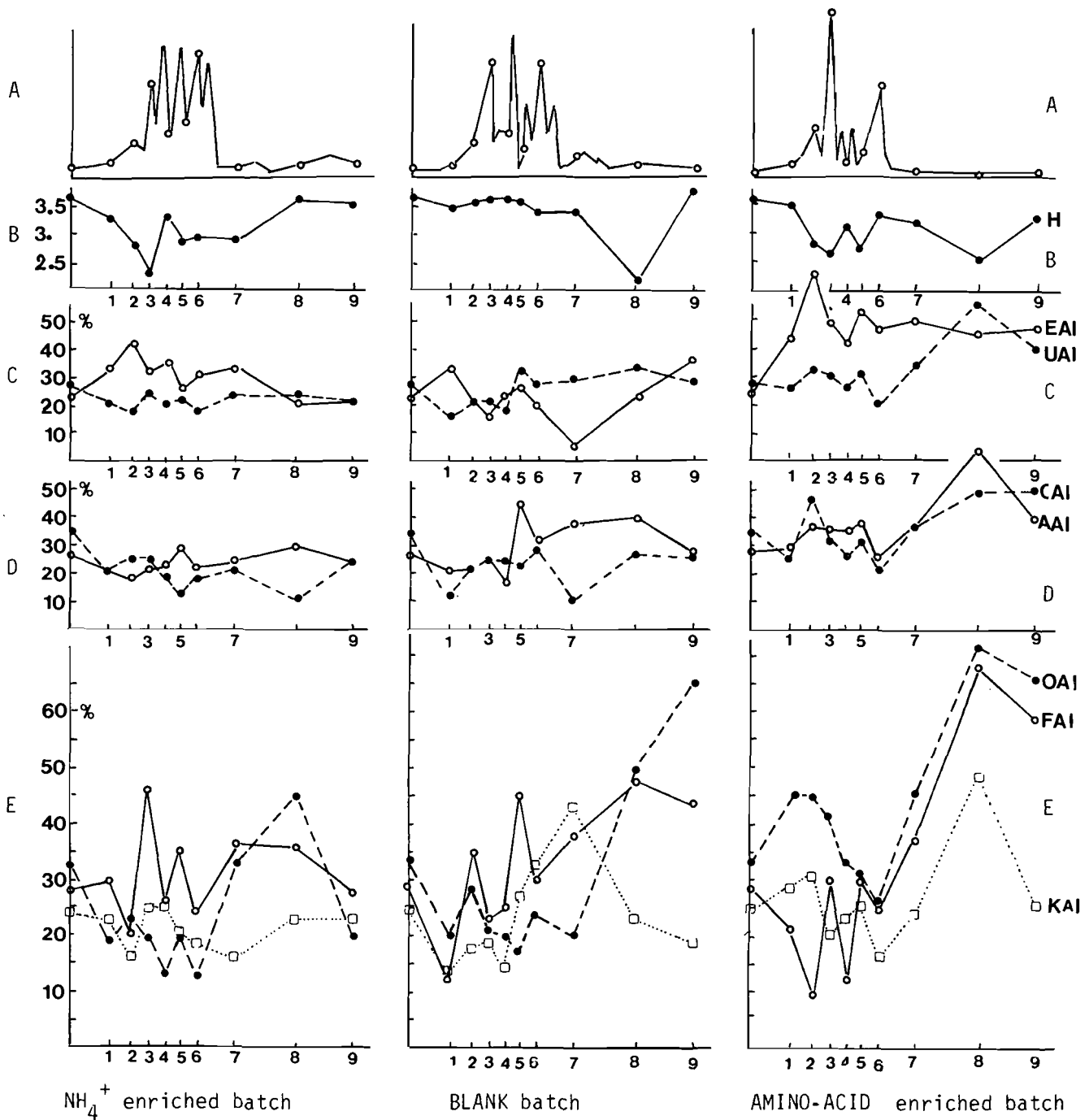


Fig. 7. Diversity index and catabolic potentialities in the 3 batches. (A) Plate-count curve pattern to show the different time samples chosen; abscissa: time samples, as in Table 1. (B) Shannon diversity index; maximum theoretic value for 20 strains (4.32) is obtained at T9 in the blank batch. (C) Exoenzyme average index (EAI, ○) and average index utilization for the 38 compounds tested as sole source of carbon and energy (UAI, ●). (D) Carbohydrates (CAI, ●) and amino-acid (AAI, ○) average utilisation indexes. (E) Alcohols (OAI, ●), fatty acids (FAI, ○) and organic-acid (KAI, □) average utilization indexes

the amino-acid enriched batch, whereas there was no significant fluctuation of the Shannon index in the blank batch (between 4.22 and 3.82). Following protozoan growth (5 to 7 d), a further decrease of Shannon index was noticed in the blank batch (at T7).

Physiological indexes

Catabolic potentialities, which considered all strains of a sample and different families of tested small organic compounds were plotted in Fig. 7. These per-

centages reflect the effect of the enrichment source and show the succession of the different nutritional potentialities during the experiment. In the 3 batches we observed, from T0, a gradual increase of chemical group utilization percentages. At the end of the experiment large differences were noted for nutritional index values of the 3 batches (Fig. 7d, e). These nutritional capacities – not commonly used in ecological work (Hauxhurst et al. 1981) – showed a specialization of the community which was not reflected by the synthetic Shannon index value.

Growth factor requirements slowly increased from the beginning of exponential growth (T2) to T6, where 55 % of the isolated strains could grow only with supplemented amino acids and/or vitamins. After T6, these requirements drastically dropped (0 %, when the number of flagellates reached a maximum).

Time evolution of bacteria in each batch

Dendrograms resulting from the hierarchical classification of the 200 strains from each batch (enriched, control, blank) show a breakdown of the entering strain curves at 0.007 taxonomic distance. On Fig. 8, 9 & 10, all strains clustering at less than 0.007 taxonomic distance are represented by triangles. As this taxonomic distance gave a high number of clusters, we decided to use an 0.05 taxonomic distance (about half of the scale on Fig. 8, 9 & 10), that would only separate a few groups of strains.

In the enriched batch, 4 groups of bacterial strains clustered at an 0.05 taxonomic distance (Fig. 8). Three of them (A, B & D groups) were already formed at a taxonomic distance of 0.03, displaying good intraphenic homogeneity. These 3 groups clustered at the 0.09 level only, showing much interphenic heterogeneity.

The 51 strains clustered in Group A had growth factor requirements, such as amino acids or vitamins. Nutritional versatility was, consequently, very limited (especially amino acid and organic acid utilization). Catabolism (production of exoenzymes) characterized this group (EAI 60 %): phosphatase, esculine, amylase and urease were the most widely produced. The strains of Group A mainly comprise pseudomonads (89 %). Amino acid enrichment played the role of a growth factor source for this population during bacterial development (T0 to T6).

The 63 strains of Group B characterized the microbial population directly concerned with amino acid enrichment. While UAI and EAI values were about the same (45 %), this population was specialized in the utilization of a few, but constant, organic compounds. Amino acids (proline, serine, aspartate, glutamate, asparagine, lysine) and gluconate were systematically used as the sole source of carbon and energy; esculine, amylase and phosphatase were regularly produced by the strains of Group B. This population, considered as the pioneers of microbial production, occurred at T2 to T3 (Table 3).

Following the bacterial bloom, we isolated the

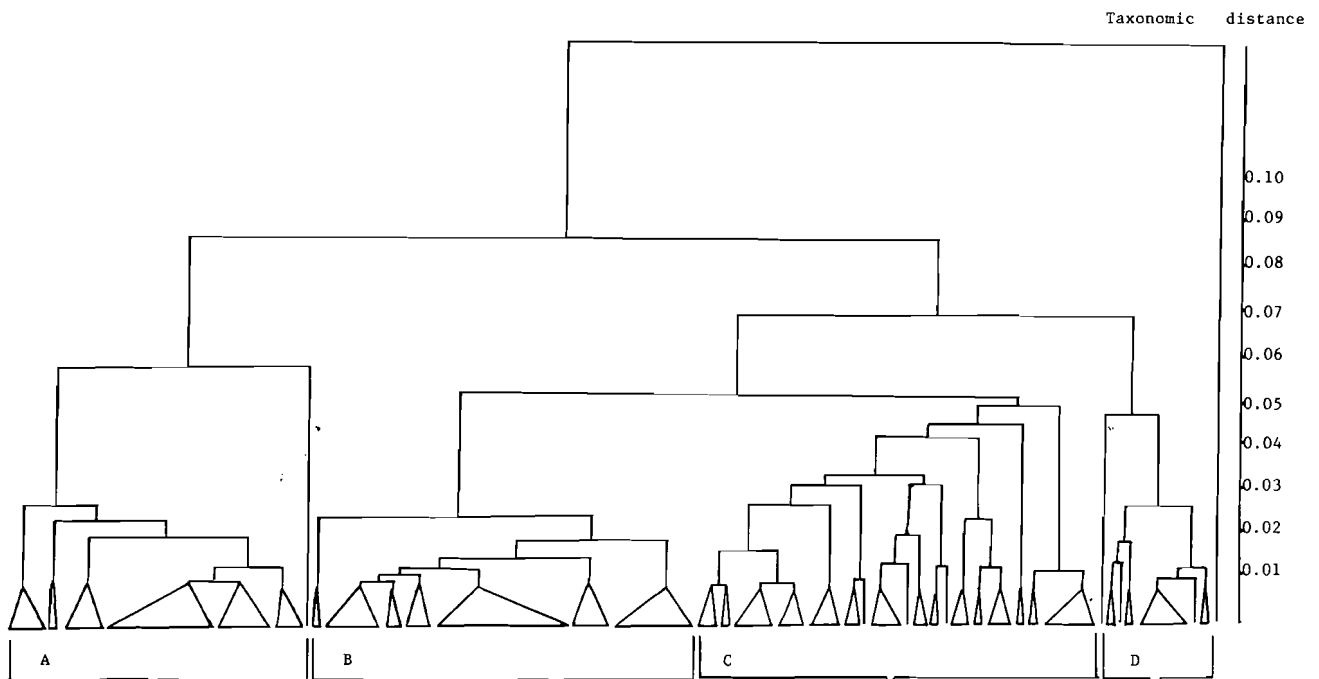


Fig. 8. Hierarchical classification of the 200 strains isolated from the amino-acid enriched batch. Triangles: clusters of more than 2 strains with 0.007 similarity level. Base length of triangles is proportional to the number of strains included in the cluster

heterogeneous strains comprising Group C. Between 0.007 and 0.05 taxonomic distance (Fig. 8), the dendrogram looked like a single linkage clustering dendrogram, i.e. many small clusters aggregated along the distance scale. This reflects the diversity of the bacterial population isolated between T7 and T9 (during and after protozoan growth). Each individual cluster exhibited different and complementary physiological abilities: exoenzyme production, growth-factor

requirements or ability to grow on amino acids and alcohols.

Group D contained 90 % of the strains isolated in the T0 sample (Table 3). This shows the rapidity and the extent of the qualitative response of heterotrophic bacteria during the lag phase just after initial enrichment.

In the control batch, heterotrophic bacterial succession was more progressive. Five main groups – A, B, C, D and E – were found at a taxonomic distance of 0.05 (Fig. 9). The effect of initial NH₄⁺ enrichment was not as marked as in the AA enriched batch, since the T0 isolated strains were mixed in Group B with some T1 and T2 strains. Group B characterized a microbial population at the beginning of the experiment (Table 4). Thereafter, during the bacterial growth phase, Group E strains predominated. The main physiological potentiality was the production of exoenzymes (EAI 52 %), such as phosphatase, amylase and DNase. These were certainly suitable for degrading particulate matter, the main source of carbon in this batch.

Thereafter, a succession of heterotrophic communities occurred from Group C (centered on Sample T4, at the end of bacterial growth) to Group A (during protozoan growth, T7 and T8). Both groups exhibited similar physiological features (EAI 19 %, UAI 20 %), in addition to complementary aspects of physiological growth capacities. They were able to grow without NaCl (Group A), or at a high salinity level (100‰: Group C), at 37° (Group A), at 4°C (Group C), and also to reduce nitrate (Group C). This feature was also observed for exoenzyme production: lecithine and gelatinase in Group A and phosphatase in Group C. For

Table 3. Amino-acid enriched batch. Origin of strains belonging to the 4 clusters formed at the 0.05 similarity level in the dendrogram presented in Fig. 8

Groups	A	B	C	D	Isolated strains
Number of strains in each group	51	63	66	18	2
Percentage of strains corresponding	25.5 %	31.5 %	33 %	9 %	
Number of strains in each sample					
T0	0	0	2	18	
T1	8	5	6	0	1
T2	7	10	3	0	
T3	7	10	3	0	
T4	6	7	7	0	
T5	8	8	4	0	
T6	11	5	3	0	1
T7	3	4	13	0	
T8	1	7	12	0	
T9	0	7	13	0	

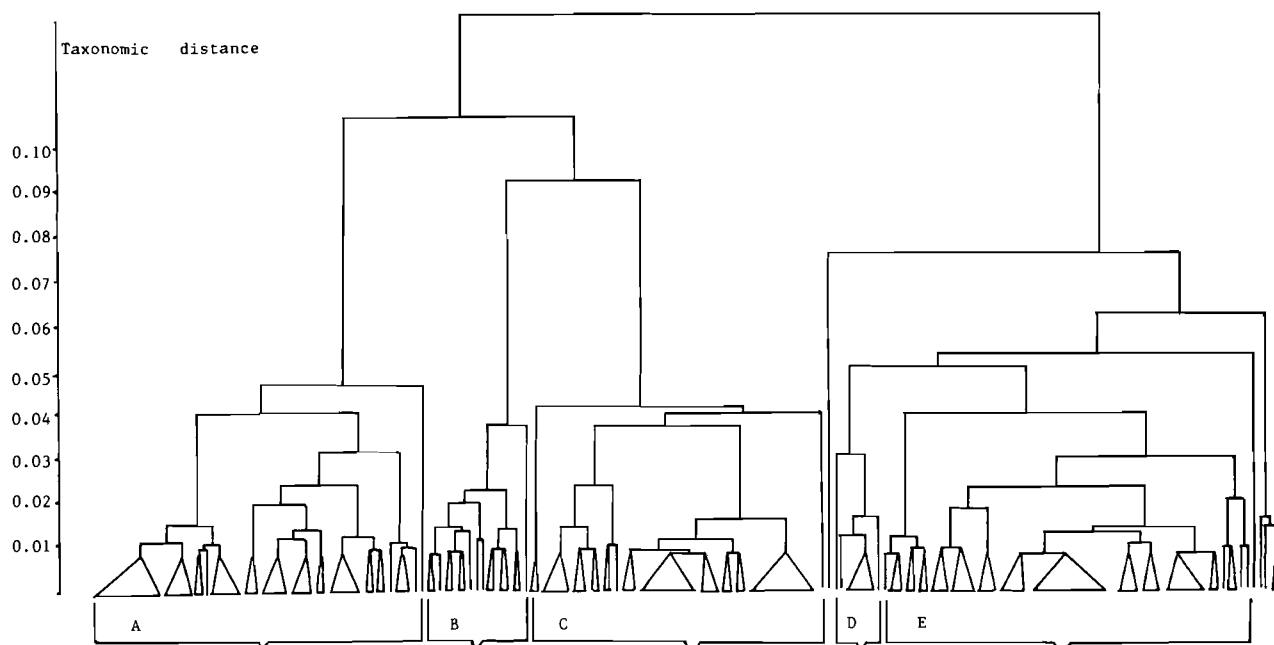


Fig. 9. Hierarchical classification of the 200 strains isolated from the NH₄⁺ enriched batch (control batch)

Table 4. NH_4^+ enriched batch. Origin of strains belonging to the 5 clusters formed at the 0.05 similarity level in the dendrogram presented in Fig. 9

Groups	A	B	C	D	E	Isolated strains
Number of strains in each group	60	17	49	8	60	6
Percentage of strains corresponding	30 %	8.5 %	24 %	4 %	30 %	3 %
Number of strains of each sample						
T0	0	11	2	4	1	2
T1	6	2	4	1	6	1
T2	5	1	2	2	10	
T3	7	0	3	0	10	
T4	1	0	13	0	5	
T5	7	0	9	0	4	
T6	6	0	7	0	7	
T7	10	0	1	0	7	2
T8	11	2	3	1	3	
T9	7	1	5	0	7	

organic compounds, amino acids were more intensively used by Group C strains, while it were the fatty acids for Group A strains.

In the blank batch, only 40 % of the isolated strains were clustered at the taxonomic distance 0.007 (Fig. 10), documenting the heterogeneity of the bacterial communities in the experiment. At a taxonomic distance of 0.05, 3 main groups (A, B & C) appeared (Table 5). Group A only comprised strains isolated at sampling times T0, T8 and T9 which did not show plate-count increase. The uniformity of Group B centering on the T7 sample (Table 5) was due to low EAI (16 %) and low nutritional versatility (UAI 37 %).

It seems that in this batch no component of the bacterial community was able to take the advantage of growth stimulation due to the wall effect.

DISCUSSION

At the beginning of the experiment, the particulate matter C/N ratio was 17 (Table 6), characteristic of non-degraded particulate matter. The decrease of the C/N ratio from 17 to 7 and 8 showed the progressive increase of bacterial biomass measured with particles on the Whatman filter. Fenchel & Jørgensen (1977) already established this nitrogen enrichment of particulate matter during degradation by bacteria. In fact, the occlusion of the GF/C Whatman filter pores during filtration allowed retention of free-living bacterial cells. This phenomenon was enhanced by the increase in size of cells and aggregates formed during the growth phase, as observed by epifluorescence microscopy.

During Day 1, a net increase in particulate organic nitrogen occurred (Table 6). At the same time, no particulate carbon increase was noticed, meaning that particle mineralization (CO_2) and bacterial carbon (biomass) retention were equivalent. A rapid increase in particulate carbon was observed on Day 2 (Fig. 5) in the batch containing dissolved organic nitrogen (enriched batch). As the measured C/N ratio included microbial biomass in addition to the organic material undergoing decomposition, the real change over time of the particulate matter C/N ratio is not clear. Presence or absence of inorganic nitrogen did not seem to influence the regular increase in particulate nitrogen, nor did it influence the measured C/N ratios. The ability of bacterial communities to utilize particulate organic matter was clearly shown in all batches by an EAI (exoenzyme production) value increase at T1 (1 d 12 h) and T2 (2 d 6 h). Parnas (1974) demonstrated, in a decomposition model in soils, that with inorganic nitrogen, the initial high C/N ratio of particulate matter decreases with time, while without NH_4^+ it increases with time.

From the qualitative point of view bacterial communities reacted within a few hours. The strains isolated at T0 clustered together, and separately so from the strains of other samples (Fig. 9 to 11). The decrease of the Shannon index observed in enriched and control batches (Fig. 7b) confirmed the specialization of the bacterial community in these batches.

For the amino-acid enriched batch, during bacterial growth (until T6: 4 d 3 h), 2 main heterotrophic populations were present simultaneously. The first (Group B; Fig. 8) was able to use amino acids as energy and carbon sources from the enrichment (high AAI values),

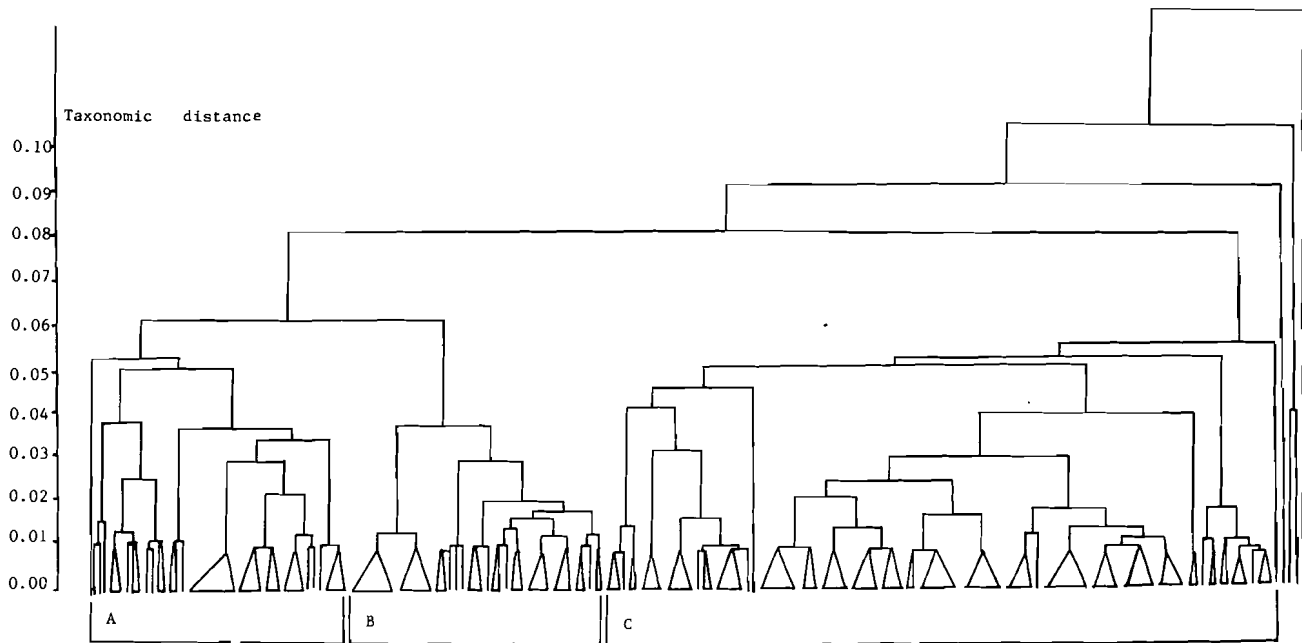


Fig. 10. Hierarchical classification of the 200 strains isolated from the blank batch

Table 5. Blank batch. Origin of strains belonging to the 3 clusters formed at the 0.05 similarity level in the dendrogram presented in Fig. 10

Groups	A	B	C	Isolated strains
Number of strains in each group	44	42	110	4
Percentage of strains corresponding	22 %	21 %	55 %	2 %
Number of strains in each sample				
T0	9	2	9	
T1	1	0	19	
T2	3	3	14	
T3	1	1	16	2
T4	1	2	17	
T5	1	8	11	
T6	1	4	15	
T7	0	15	4	1
T8	13	3	4	
T9	14	4	1	1

while the second (Group A), being able to use macromolecules (high EAI values), utilized C and N organic enrichments (dissolved amino acids) as a growth-factor source. The percentage of auxotrophic strains increased gradually from T1 to T6, suggesting that auxotrophic bacteria proliferated more during the bacterial growth phase. Group A disappeared immediately after predation started.

For the blank batch, the results demonstrated a 'wall effect' which permitted only a small increase in bacte-

rial numbers. In contrast to amino acids or NH_4^+ enriched batches, there was no mixing of strains of different origin (Fig. 10), reflecting the absence of a dominant ecotype in the experiment. For the diversified community of the blank batch, physiological indexes reflected only the average response of a bacterial community made up of different exotypes.

The microflagellates grew exponentially from 4 d 15 h to 5 d 15 h. The calculated growth rate for flagellates was 0.073 h^{-1} (correlation coefficient 0.96 on 5 points). Our 350 l batches involved a clearance of about $710^{-7} \text{ ml flagellate}^{-1} \text{ h}^{-1}$. Such a low value, compared to that of Fenchel (1982), was probably due to the small size ($8 \mu\text{m}^3$) of the flagellate. During this period, the grazing rate decreased gradually from 12 to 0.7 bacteria eaten $\text{flagellate}^{-1} \text{ h}^{-1}$. The gross growth efficiency in biovolume was $(80 \times 10^3 \times 8.7) / (30 \times 10^6 \times 0.1) \times 100 = 23 \%$, a value within the range reported previously (Fenchel, 1982, Sherr et al. 1983).

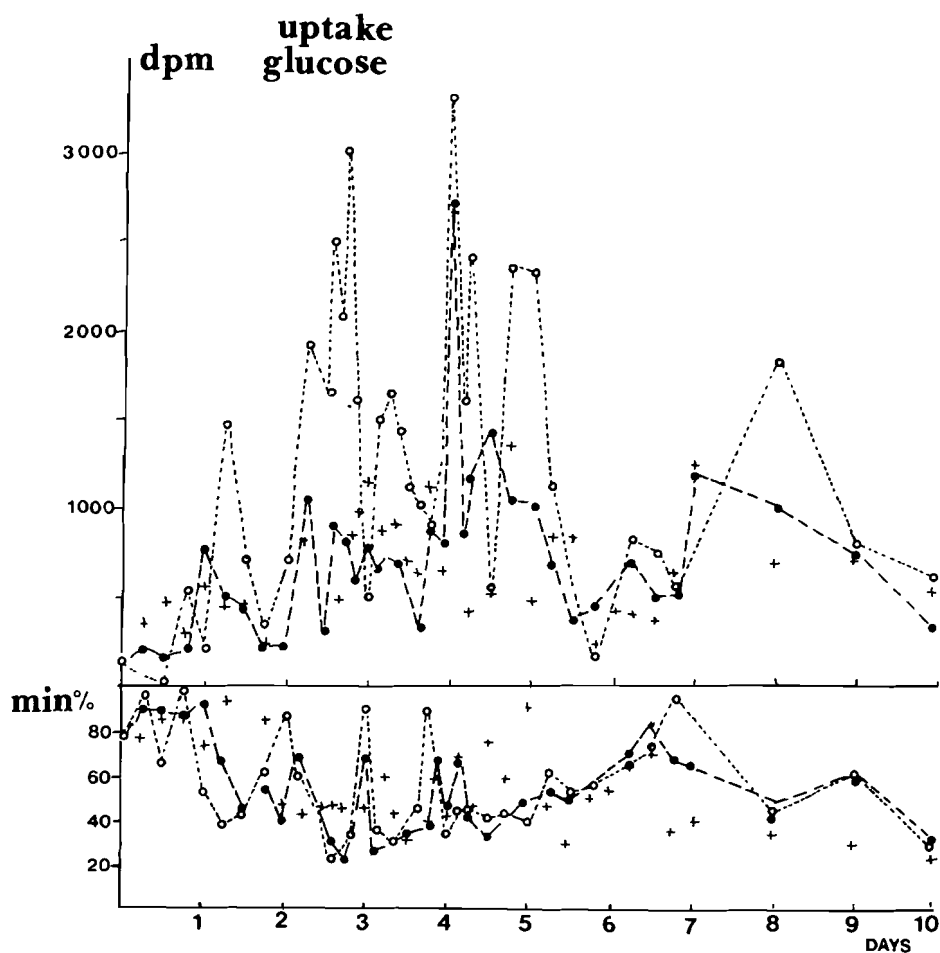
Gude (1979) noticed a decreasing suitability of activated-sludge bacterial populations as food organisms for protozoans. This was due to an increase in bacterial size (filamentous, spiral or floc forms larger than the protozoans). But there could have been also a direct interaction such as excretion of substances stimulating bacterial populations. In our experiment, during exponential growth of flagellates, the average utilization percentage of alcohols, fatty acids (in all 3 batches) and organic acids (except the control batch) increased. This trend continued after protozoan growth (T7 to T8: 8 d) and showed a high specialization in the constant use of a few, small organic compounds.

Table 6. C/N ratios of particulate matter in the 3 batches

Incubation time (days)	0	1	2	3	4	5	6	7	8	9	10
Blank batch	16.9	13.9	10.5	9.2	8.1	8.5	8.9	8.9	8.6	13.4	12.3
NH ₄ ⁺ enriched batch		13.7	13.0	9.7	9.1	7.9	8.4	8.3	8.4	9.8	7.9
Amino-acid enriched batch		10.7	9.3	7.8	7.5	7.2	7.8	7.5	7.5	7.7	7.6

Table 7. Elements for calculation of ammonium mineralization rates

Time period	Number of cells; N = average value extrapolated	NH ₄ ⁺ mineralized	Average cell volume	NH ₄ ⁺ excreted cell ⁻¹ h ⁻¹	NH ₄ ⁺ excreted mg dry wt h ⁻¹
	Bacteria ml ⁻¹	μg-at N l ⁻¹	μm ³	μg-at N bacterium ⁻¹ h ⁻¹	μg-at N mg dw ⁻¹ h ⁻¹
From 2 d 6 h to 2 d 21 h (15 h)	1 × 10 ⁶ 30 × 10 ⁶ N = 8.5 × 10 ⁶	0 8	0.1	6.2 × 10 ⁻¹¹	2.7
	Flagellates ml ⁻¹	μg-at N l ⁻¹	μm ³	μg-at N flagellate ⁻¹ h ⁻¹	μg-at N mg dw ⁻¹ h ⁻¹
From 4 d 18 h to 5 d 6 h (12 h)	13.8 × 10 ³ 80 × 10 ³ N = 37.6 × 10 ³	4 13.8	8.7	2.2 × 10 ⁻⁸	10

Fig. 11. Amino-acid uptake and corresponding mineralization percentage in the NH₄⁺ enriched batch (---), amino-acid enriched batch (...) and blank batch (+)

Selective action of microflagellates was also observed on ^{14}C glucose, a ^{14}C amino-acid mixture, and in respiration curves (Fig. 11 & 12). There was a positive effect of glucose uptake during exponential growth of flagellates and the effect on amino-acid uptake was noticeable after protozoan growth. Amino-acid respiration percentages remained around 5 to 10% until the end of the experiment, showing a sudden high efficiency in amino-acid assimilation. Sherr et al. (1982) explained the selective action of microflagellates on carbohydrate mineralization by an enhancement in the rate of mineral cycling, especially phosphorus. In their experiment, the C/N ratio was higher than the C/N amino-acid ratio used here, but phosphorus was indeed a limiting nutrient in our experiment, and a new increase in particulate phosphorus from Day 6 to Day 8 was observed.

Considering exoenzyme production, DNase was noticed in the control and in the enriched batches during the experiment, while this enzyme appeared in the blank batches at T8 and T9 only, suggesting a non-neglectable part of natural mortality in flagellate disappearance *versus* predation by ciliates.

Furthermore, if the erratic presence of urease from strains isolated at T8 and T9 suggested the presence of urea in all batches, NH_4^+ was the most extensive form of nitrogen excretion for flagellates (Paashe & Kristiansen 1982). Indeed, NH_4^+ curves showed a peak of flagellate growth between Day 5 and Day 6.

From direct counts, the NH_4^+ mineralization curve, and the disappearance of NH_4^+ in the control, mineralization rates of both heterotrophic populations (Table 7) were estimated. Considering volume/dry-weight conversion errors and NH_4^+ estimated values, mineralization rates were about the same, i.e. 2.7 and $10\ \mu\text{g-at N-NH}_4^+1^{-1}\text{mgdw}^{-1}\text{h}^{-1}$ for bacteria and flagellates, respectively. These values are much higher than the daily rates estimated *in vivo* with the ^{15}N dilution techniques (Caperon et al. 1979, Paashe & Kristiansen 1982), but they reflect local responses of heterotrophic communities under favoured growth conditions. These numbers also show that microheterotrophic flagellates played as important a role as did the bacteria for regenerating nutrients.

Acknowledgments: This work was supported by EEC Grant ENV-699-F.

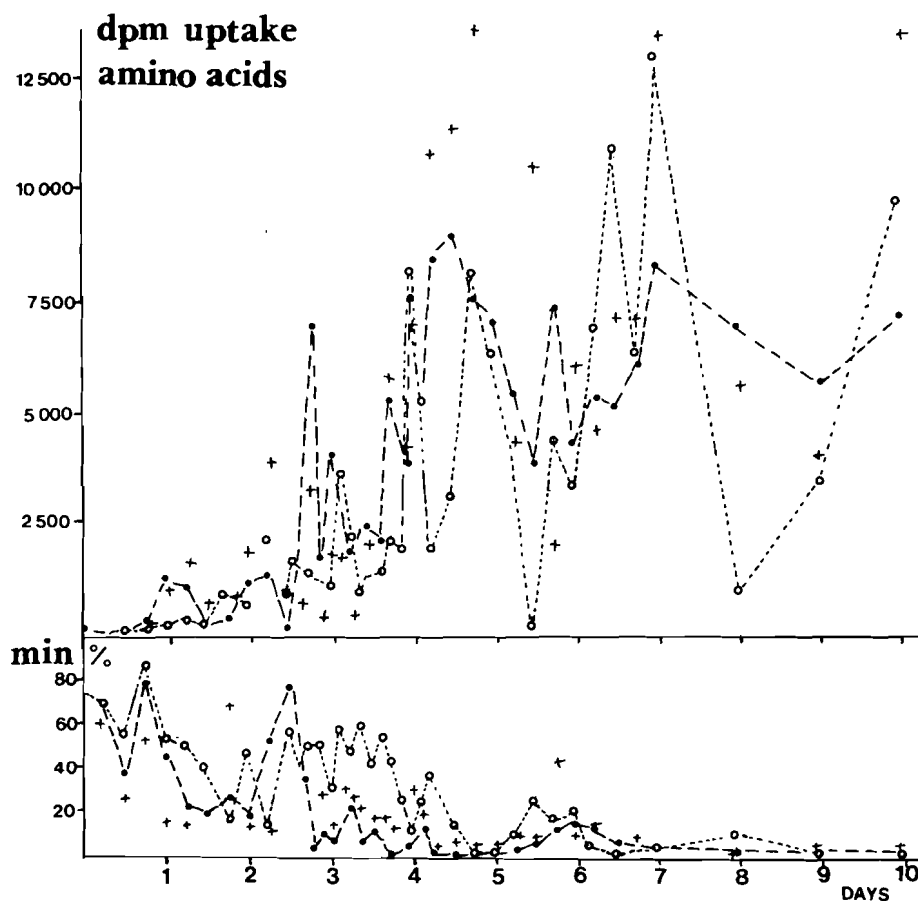


Fig. 12. Glucose uptake and corresponding mineralization percentage in the NH_4^+ enriched batch (---), amino-acid enriched batch (...) and blank batch (+)

LITERATURE CITED

- Amano, M., Hara, S., Taga, N. (1982). Utilization of dissolved amino acids in sea water by marine bacteria. *Mar. Biol.* 68: 31–36
- Bianchi, M. A., Bianchi, A. J. M. (1982). Statistical sampling of bacterial strains and its use in bacteria diversity measurements. *Microb. Ecol.* 8: 61–69
- Bright, J. J., Fletcher, M. (1983). Amino acid assimilation and electron transport system activity in attached and free-living bacteria. *Appl. environ. Microbiol.* 45 (3): 818–825
- Caperon, J., Schell, D., Hirota, J., Laws, E. (1979). Ammonium excretion rates in Kaneohe Bay, Hawaii, measured by an ¹⁵N isotope technique. *Mar. Biol.* 54: 33–40
- Delabre, M., Bianchi, A., Veron, M. (1973). Etudes critiques de méthodes de taxonomie numérique. Application à une classification de bactéries aquicoles. *Ann. Microbiol. Inst. Pasteur.* 124 A: 489–506
- Fenchel, T. (1982). Ecology of heterotrophic microflagellates. II. Bioenergetics and growth. *Mar. Ecol. Prog. Ser.* 8: 225–231
- Fenchel, T. M., Jørgensen, B. B. (1977). Detritus food chain of aquatic ecosystems: the role of bacteria. In: Alexander, M. (ed.) *Advances in microbial ecology*. New York, p. 1–49
- Frost, B. W. (1972). Effect of size and concentration of food particles on the feeding behavior of the marine planktonic copepod *Calanus pacificus*. *Limnol. Oceanogr.* 17: 805–815
- Graham, J. M., Canale, R. P. (1982). Experimental and modeling studies of a four trophic level predator-prey system. *Microb. Ecol.* 8: 217–232
- Gude, H. (1979). Grazing by Protozoa as a selection factor for activated sludge bacteria. *Microb. Ecol.* 5: 225–237
- Heinbokel, J. F. (1978). Studies on the functional role of tintinnids in the southern California Bight. I. Grazing and growth rates in laboratory cultures. *Mar. Biol.* 47: 177–189
- Hauxhurst, J. D., Kaneko, T., Atlas, R. M. (1981). Characteristics of bacterial communities in the Gulf of Alaska. *Microb. Ecol.* 7: 167–182
- Hobbie, J. E., Daley, R. J., Jasper, S. (1977). Use of nucleopore filters for counting bacteria by fluorescence microscopy. *Appl. environ. Microb.* 37 (5): 805–812
- Hollibaugh, J. T., Carruthers, A. B., Furhman, J. A., Azam, F. (1980). Cycling of organic nitrogen in marine plankton communities in enclosed water columns. *Mar. Biol.* 59: 15–21
- Iturriaga, R., Zsolnay (1981). Transformation of some dissolved organic compounds by a natural heterotrophic population. *Mar. Biol.* 62: 125–129
- Krambeck, C., Krambeck, K. H. J., Overbeck, J. (1981). Microcomputer assisted biomass determination of plankton bacteria on scanning electron micrographs. *Appl. environ. Microbiol.* 42 (1): 142–149
- Laake, M., Dahle, A. B., Eberlein, K., Rein, K. (1983). A modelling approach to the interplay of carbohydrates, bacteria and non-pigmented flagellates in a controlled ecosystem experiment. *Mar. Ecol. Prog. Ser.* 14: 71–79
- Mills, A. L., Wassel, R. A. (1980). Aspects of diversity measurements for microbial communities. *Appl. environ. Microbiol.* 40: 578–586
- Oppenheimer, C. H., ZoBell, C. E. (1952). The growth and viability of sixty-three species of marine bacteria as influenced by hydrostatic pressure. *J. mar. Res.* 11: 10–18
- Paashe, E., Kristiansen, S. (1982). Ammonium regeneration by microzooplankton in the Oslofjord. *Mar. Biol.* 69: 55–63
- Parnas, H. (1974). Model for decomposition of organic material by microorganisms. *Soil. Biol. Biochem.* 7: 161–169
- Sepers, A. B. J. (1981). Diversity of ammonifying bacteria. *Hydrobiologia* 83: 343–350
- Sherr, B. F., Sherr, E. B., Berman, T. (1982). Decomposition of organic detritus: a selective role for microflagellates protozoa. *Limnol. Oceanogr.* 27: 765–769
- Sherr, B. F., Sherr, E. B., Berman, T. (1983). Grazing, growth and ammonium excretion rates of a heterotrophic microflagellate fed with four species of bacteria. *Appl. environ. Microbiol.* 45 (4): 1196–1201
- Strickland, J. D. H., Parsons, T. (1968). A practical handbook of sea water analysis. *Bull. Fish. Bd Can.* 167
- Van Wambeke, F., Bianchi, M. (1985). Dynamics of bacterial communities and qualitative evolution of heterotrophic bacteria during the growth and decomposition processes of phytoplankton in an experimental marine ecosystem. *J. exp. mar. Biol. Ecol.* 60: in press
- Van Wambeke, F., Bianchi, M. A., Bianchi, A. J. M. (1983). Dynamique des communautés bactériennes d'une eau lagunaire enrichie en azote. *Oceanol. Acta. Proc. int. Sym. on Coastal Lagoons, Bordeaux.* 8–14 September 1981
- Van Wambeke, F., Bianchi, M. A. (1985). Bacterial biomass production and ammonium regeneration in Mediterranean sea water supplemented with amino acids. 1. Correlations between bacterial biomass, bacterial activities and environmental parameters. *Mar. Ecol. Prog. Ser.* 23: 107–115
- Yentsch, C. S., Menzel, D. W. (1963). A method for the determination of phytoplankton chlorophyll and phaeophytin by fluorescence. *Deep Sea Res.* 10: 221–231

This paper was presented by Professor G. Rheinheimer; it was accepted for printing on February 11, 1985